

Laboratory investigation of the impact force of debris flow on a passable structure

Analyse en laboratoire de la force d'impact d'une coulée de débris sur une structure 'franchissable'

A. L. Yifru

Department of Civil and Environmental Engineering/Norwegian University of Science and Technology, Trondheim, Norway

H. Vicari, S. Nordal, V. Thakur

Department of Civil and Environmental Engineering/Norwegian University of Science and Technology, Trondheim, Norway

ABSTRACT: In mountainous regions, debris-flow is one of the natural hazards imposing threats to human lives and infrastructures. In order to estimate the magnitude of its destructive force, a number of empirical and analytical formulas are presented in the literature. In addition, laboratory investigations on rigid and flexible barriers are also presented. Most of the laboratory tests are conducted by blocking the entire flow of the debris. However, debris flow could pass by the sides of structures after hitting them. In this study, the impact force of debris-flow on a rectangular pillar that functions as a passable rigid barrier is investigated in a laboratory flume model. The flume model has a 0.3m wide, 6m long run-out channel and a 2.2m wide, 4m long deposition area. A 25mmX50mm rectangular hollow steel pillar equipped with a load cell is placed at the end of the run-out channel representing a passable structure. Series of impact tests are conducted with three different total volumes, V (25, 30, and 35 litres), and three solids concentrations, C_s (60%, 55%, and 50%) that resulted in varying discharges of debris flow mixture. The solid part is a natural sand aggregate with different grain size distribution, GSD ($G1$, $G2$, and $G3$). From conservation of momentum, unit impact pressure computed by multiplying the bulk density, discharge and front velocity is seen to fit with the recorded impact pressure with a correction value of $k \approx 0.9$ to be applied for this passable structure case. It is also shown that the Froude number, F_r , and the resulting normalized impact pressure, P_{norm} are influenced by the choice of GSD (fine content) and C_s (water content) where higher fine and water content result in higher F_r and lower P_{norm} .

RÉSUMÉ: Dans les régions montagneuse, les coulées de débris sont parmi les dangers naturels qui menacent la vie des personnes et les infrastructures. Afin d'estimer la magnitude de sa force destructive, différentes formules empiriques et analytiques sont présentées dans la littérature. Des études de laboratoire sur des barrières rigides et flexibles sont également présentées. La plupart des tests de laboratoire sont effectués en bloquant complètement le flux de débris. Cependant, une coulée de débris pourrait passer par les côtés des structures après les avoir heurtées. Dans cette étude, la force d'impact de la coulée de débris sur un pilier rectangulaire servant de barrière rigide est étudiée en laboratoire à l'aide d'essais en chenal. Les dimensions du chenal sont 0,3 m de large et 6 m de longueur; la surface de dépôt est 2,2 m de large et 4 m de longueur. Un pilier rectangulaire en acier creux de 25 mm x 50 mm équipé d'un capteur de force est placé à l'extrémité du chenal représentant une structure franchissable. Pour chacun des essais, 3 volumes total de débris (V) ont été utilisés (25, 30 et 35 litres) ainsi que

3 concentrations de solides, C_s (60%, 55% et 50%). Ces concentrations et volumes ont entraîné des débits variables lors des essais au laboratoire. La partie solide est un agrégat de sable naturel avec différentes distributions granulométriques. À partir de la conservation de la quantité de mouvement, la pression d'impact unitaire calculée en multipliant la densité du flux de débris, son débit et sa vitesse est corrélée à la pression d'impact enregistrée en utilisant un facteur de correction $k \approx 0,9$ qui s'applique dans le cas d'une structure franchissable. Il est également montré que le nombre de Froude, F_r , et la pression d'impact normalisée résultante, P_{norm} , sont influencés par le choix de GSD (teneur fine) et de C_s (teneur en eau), où une teneur élevée en eau et en fine cause une augmentation de F_r et une diminution de P_{norm} .

Keywords: Debris flow, impact force, passable structures, countermeasures, flume modelling

1 INTRODUCTION

Rainfall triggered debris flow is becoming increasingly common along the fjords of Norway due to the changing climate and extreme weather events. Debris flow can travel to a greater distance posing threats to infrastructures and human lives within its reach. Therefore, structural countermeasures such as check dams, slit dams, rigid barriers or flexible barriers are often implemented as risk reduction strategy. Among others, the impact force of debris flow on countermeasures is one of the issues being studied extensively in literature; theoretically (e.g. (Armanini 1997; Mizuyama 1979)) from field observations (e.g. (Zhang 1993; Arattano and Franzini 2003)), and laboratory testing (e.g. (Hübl and Holzinger 2003; Zanuttigh and Lamberti 2006; Tiberghien et al. 2007; Huang, Yang, and Lai 2007; Scheidl et al. 2013)). However, majority of these laboratory studies are either conducted using granular flows and/or used full flow blocking mechanism to measure the impact force.

A complete stoppage of debris flow may not always be possible, in particular, along the fjords where the mountains are very steep. One effective solution could be to channelize the debris flow to the fjord using deflection walls and underpasses where passable countermeasures will be considered appropriate. However, to ensure a safer passage, it requires that the passable countermeasures can sustain the impact forces induced by moving debris. Recently, some field

and laboratory scale tests that captured the interaction between debris flows and passable structures are given in literatures (e.g. (Cui, Zeng, and Lei 2015; Nagl, Kaitna, and Hübl 2018; D. Wang et al. 2018; Y. Wang et al. 2018)).

This work is inspired by the Norwegian conditions and attempts have been made to study the impact forces on passable structures such as bridge pillar. The results are discussed in comparison with those found in literatures to validate the impact force measurement method presented here. In addition, investigation of the debris flow characteristics or constituents [i.e. change in Grain size distribution (GSD) in terms of fine content, total release volume (V) and solids concentrations by volume (C_s)] are investigated for their influence in the resulting impact pressure on passable structures.

2 METHODOLOGY

Flume model testing has been adopted by several researchers to understand different flow mechanisms and properties of debris flows as field testing is relatively expensive. In this study, laboratory flume model testing is used.

2.1 The flume model

The flume model used in this study has a total of 10m which constitutes a 6m long run-out channel and a 4m long deposition area (see Figure 1). The run-out channel has an adjustable width and

slope. For this study, 30cm channel width and 17° fixed 2° slope with 2.2m wide space. slope angle are used. The deposition area has a

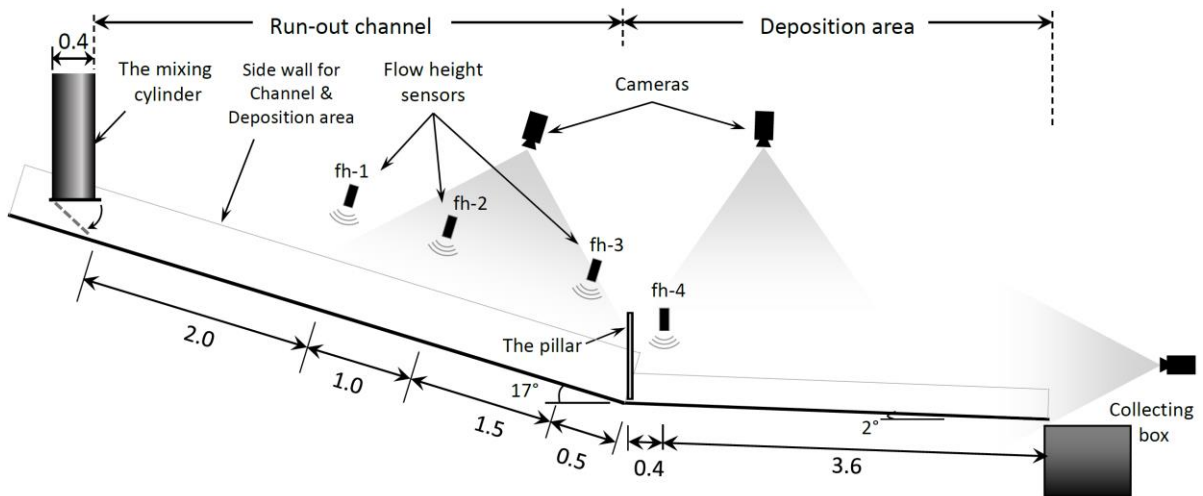


Figure 1: The flume model profile view (All dimensions in meters)

Four flow height sensors (MIC+35/IU/TC Ultrasound), three in the run-out channel and one at the start of the deposition area are installed. A load cell (S2M Force Transducer) is attached at the top of the pillar and the pillar is installed at the end of the run-out channel.

A data acquisition software is custom made using LabVIEW2018 software to record flow height changes in different locations of the channel and impact force on the rectangular pillar from the sensors and the force transducer. Rate of data recording is 50Hz.

Four video cameras were used. Two 120fps recording cameras were used in the run-out channel and deposition area while one 60fps capacity camera was used in front of the model to capture the overview of the test. One high speed camera with 1000fps recording capacity was used in different locations to closely study the debris flow behaviour and impact mechanism. The high speed video also assisted in determining the flow front velocity, v , approaching the pillar.

The debris releasing container is a vertical cylinder equipped with a motor and a rotating mixing arm. This enables thorough mixing of the soil-water mass inside the cylinder before and

upon release. This new method of mixing and releasing mechanism ensures the release of the entire homogeneously mixed soil-water mass. The resulting flow is assumed to replicate a well-developed debris flow.

2.1.1 Set-up for impact force measurement

The fundamental working principle of the force measuring pillar is the concept of torque. Torque is a product of force and perpendicular distance (so called lever-arm) from some rotation point. The set-up of the pillar, as shown in Figure 2, is placed vertically while it is secured by a circular rod in its mid-section horizontally by two frictionless bearings. A load cell is attached on its top. This placement is at equi-distance from the mid-section as the resultant debris impact location (equal lever-arm) at the bottom. The bottom end of the pillar is made to have no contact with the surface by maintaining ca. 2mm gap.

2.1.2 Boundary conditions

In this study, the model is made to simulate a well-developed debris flow in a defined sloped and smooth channel. The triggering mechanism

and initiation phase of real debris flow are not part of this test simulation. The surface (bed) friction and/or entrainment characteristic of real debris flow are not considered. The characteristics of these surfaces and the rheology of the debris material are assumed to be uniform throughout the repetition of the tests.

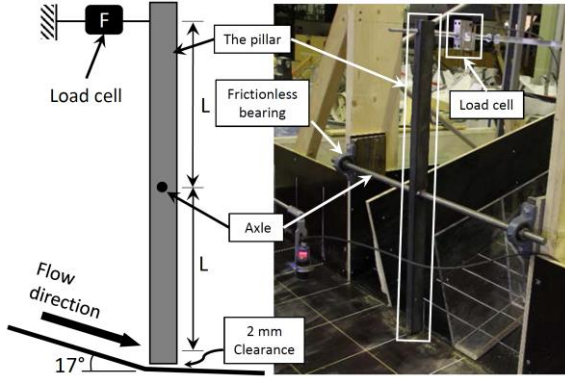


Figure 2: The force-measuring pillar: side view and photo ($L = 0.45\text{m}$) [The photo is in reverse view]

2.2 The test material

The test material, that is named $G1$, is a natural sand aggregate from Hofstad, Trondheim, Norway quarry site. GSD of $G1$ is given in Figure 3 along with its two variations ($G2$ and $G3$).

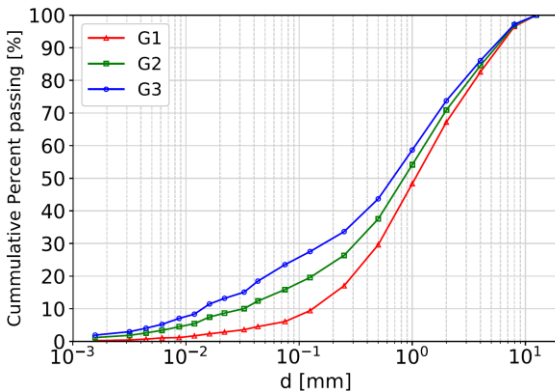


Figure 3: Grain size distribution (GSD) curves of the debris materials ($G1$, $G2$, and $G3$)

These variations are made by replacing 10% and 20% of the dry soil mass of $G1$ by its fine fraction with sizes less than 0.075mm . These variations

are intended to study the effect of fine particles in the mobility and mechanism of debris flow and its impact force.

Table 1: Important sizes and gradation properties of the debris materials (grain sizes are in mm)

	$G1$	$G2$	$G3$
d_{10}	0.13	0.03	0.01
d_{30}	0.51	0.32	0.17
d_{50}	1.05	0.88	0.68
d_{60}	1.52	1.27	1.06
d_{max}	8.00	8.00	8.00
C_u	11.69	38.48	75.71
C_c	1.32	2.44	1.95

Important sizes and gradation properties of these three materials are given in Table 1. The resulting gradation properties, coefficient of uniformity, C_u and coefficient of curvature, C_c show that all the three materials are well-graded. The particle density of the sand grains is found to be $\rho_s = 2.75$. During the repetition of the tests, the respective GSD s were maintained without any significant variation.

2.3 Test procedure

The experiments were conducted using different discharges of debris with solid-water mix having solids concentration C_s of 60% ($C1$), 55% ($C2$), and 50% ($C3$) by volume. According to (Iverson 1997), the choice of C_s determines the resulting bulk density, ρ of the debris along with ρ_s as $\rho = \rho_s \cdot C_s + \rho_w(1 - C_s)$. $C1$, $C2$ and $C3$ give 2050 kg/m^3 , 1962 kg/m^3 and 1875 kg/m^3 of ρ respectively. The variation in discharge is achieved by varying the V between 25L ($V1$), 30L ($V2$) and 35L ($V3$).

A weighed amount of solid and water is added in the mixing cylinder before lifting and suspending it in the releasing position using a crane. Then, the motor is started to mix the soil-water mass while making the video cameras and the

data acquisition software ready. After approximately a minute of thorough mixing, the bottom gate is opened to start the test.

After approximately 30seconds, all measurements are stopped and saved. Photos, visual observations and manual measurements are, then, taken before cleaning the model and made it ready for another test.

3 RESULTS

The recorded forces and flow heights of 27 tests are collected from their respective plots (an example from first test with *GIVICI* is shown in Figure 4). The minimum and maximum values of v , peak impact height, h_{Max} and peak impact force, F_{Max} are given in Table 2.

Table 2: Range of values recorded from the 27 tests

V [m/s]	h_{Max} [mm]	F_{Max} [N]
2.40 – 4.20	19.07 – 38.47	10.38 – 22.81

The v is calculated by tracking the flow front of the recorded video using Tracker v5.06 video analysis and modelling tool (<https://physlets.org/tracker>). The third flow height sensor (fh-3) is situated 0.5m before the pillar and used for peaking h_{Max} . During impact, the debris is seen to jump and splashed vertically against the pillar that necessitate the impact height to be measured at this position.

4 DISCUSSION

The test results obtained are analysed to show which parameter and/or behaviour of the debris flow influences the impact force more.

4.1 Relationship between discharge, Q and impact force, F_{Max}

In a previous preliminary study presented in (Yifru et al. 2018), a simple linear relationship

was given as $\bar{F}_{Max} = aQ$ that fit reasonably with the results of nine impact tests on a circular pillar. More tests are needed to validate this relationship and to evaluate the ranges of values of the multiplying factor ‘ a ’. However, since impact area and shape differs in this test, the total discharge, Q , is normalized by the blocking ratio of the pillars, w/W . where w is effective width of the pillars (0.025m for rectangular, 0.07m for circular) and W is width of the channel (0.3m).

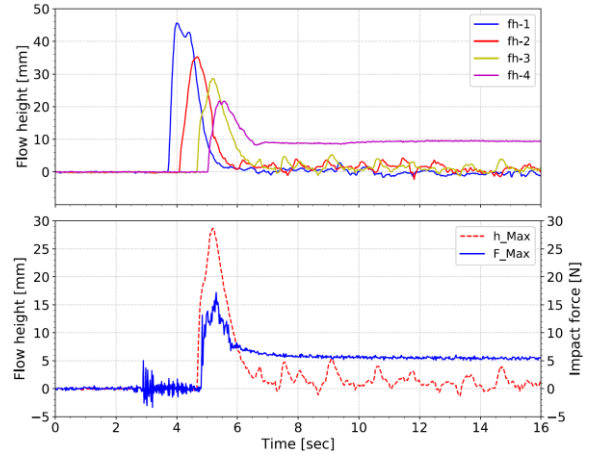


Figure 4: Typical test result (from *GIVICI*) showing flow heights and impact force plots against time

In the current test (see Figure 5), the increasing trend of peak impact force with increase of discharge is achieved. However, more scatter is observed mainly with *G2* tests. Higher v and relative higher impact forces are also observed.

Since the previous test was conducted using $C_s = 60\%$, the current test is plotted based on concentration. With one outlier from *C1* tests, the rectangular pillar respond steeply to the change of discharge than the circular one. Here it is worth noting that the slope in the previous test was 14° which might have contributed to the relatively lower v and recorded impact force. In addition, other factors like pillar shape could have contributed in the measured force. However, in this work, the effect is not taken in to account. As a result, quantifying the multiplying factor ‘ a ’, is more challenging as it is being forced to carry all

the variations in geometry and flow characteristic.

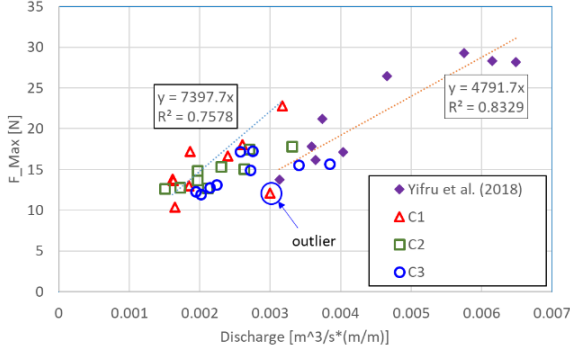


Figure 5: Relationship of discharge with the resulting peak impact force

Out of several hydrostatic and hydrodynamic impact force estimating formula evaluated, the one suggested by Mizuyama, T. (1979) that considered conservation of momentum seems to fit our test result. Equation (1) gives the relationship as:

$$p = k \cdot \rho \cdot q \cdot v \quad (1)$$

Where p is impact force per unit width in N/m, k is correction factor ($k = 1$ for Mizuyama, T. (1979)), q is the discharge per unit width ($\text{m}^3/\text{s}/\text{m}$) and v is in m/s.

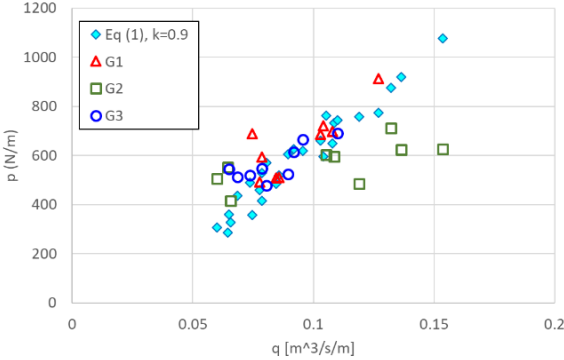


Figure 6: Impact force comparison: measured Vs calculated by Equation (1)

The type of material chosen was tested against this equation and the factor k is found to vary between 0.85 and 1.0 for the individual $GSDs$. In

general, $k \approx 0.9$ fits for the total data-set, with a $G2$ outlier, as shown in Figure 6. The k value, here, can be considered as a factor for a passable structure. The relationship given in Equation (1) used the recorded v and h_{Max} values of the test along with their respective ρ .

It is challenging to represent a complex flow of soil-water mix using a single value of flow characteristics. This leads to the use of dimensionless parameters like Froude number, F_r and normalized impact pressure, P_{norm} that employ combination of the flow parameters.

4.2 Dimensionless numbers comparison with normalized impact pressure

The dimensionless numbers, $F_r = v/\sqrt{gh}$ and the $P_{norm} = (F_{Max}/A)/\rho v^2$ where $A = w \cdot h_{Max}$, have shown to follow a power-function relationship proposed by Hübl et al. (2009). They used data from miniaturized tests and field observations found in, among others, (e.g. (Hübl and Holzinger 2003; Tiberghien et al. 2007)).

The data are plotted in the F_r Vs P_{norm} plot and presented in Figure 7. It includes three plots to show the variation according to GSD , V and C_s . Data from (Cui, Zeng, and Lei 2015; Hübl and Holzinger 2003; Yifru et al. 2018) are included to show a comparison from other miniaturized model tests. Cui, P. et.al (2015), after processing 155 sets of data, proposed a power-function trend line.

The P_{norm} from this study, generally, are seen to be higher than other data given in the plot and the proposed trend line looks to underestimate it. There might be two reasons for this: 1) the F_{Max} peaked from the plots (see Figure 4) are not averages, rather the absolute maximum values were taken; and 2) in the other data (e.g. from Cui, P. et al. (2015)), the peak impact pressure is computed from average of the bottom (at 1.5cm) and middle (at 4.5cm) vertically aligned sensors. Having said that, despite some scatter (with $R^2=0.3075$), our test gives a power-function relationship as: $P_{norm} = 5.6 \cdot F_r^{-0.93}$.

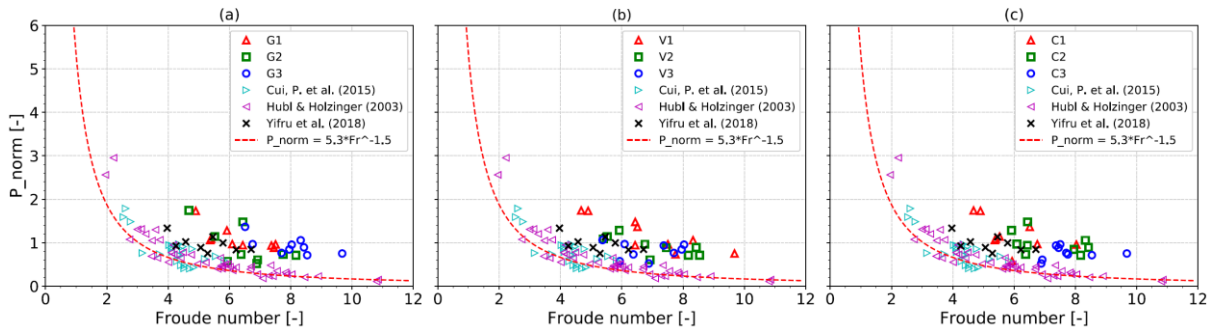


Figure 7: Froude number Vs Normalized pressure with variation based on (a) GSD, (b) Volume, and (c) Solids concentration

In comparing the results among the variations in this study, F_r is seen to carry the effect of v more than the effect of h_{Max} . Higher C_s resulted in lower value of F_r and vice versa. This influence of solid fraction (C_s) on F_r is also reported in Song et al. (2017). Fine content is also seen to influence the F_r through higher value from $G3$ and relatively lower F_r during the use of $G1$ and $G2$. Generally, higher C_s ($CI=60\%$) and lower fine content ($G1$) resulted in higher P_{norm} with lower F_r . However, the larger V is seen to result in lower P_{norm} with narrow range of F_r while the smallest V seen to result in relatively higher P_{norm} with wider range of F_r . Except the variation in F_r range, choice of V doesn't show a direct relationship with the resulting F_r value like C_s and GSD .

The flume model used in this study has smooth bed and side walls providing minimum friction. This low friction, mainly from the bed, contributed to the high v and low h_{Max} . The high v value contributes to the observed relatively high impact forces that are reflected on the calculated higher F_r and P_{norm} .

5 CONCLUSIONS

This new method of measuring impact force of debris flow is evaluated using more flume tests with varying GSD , V and C_s while assuming a possible passable structure in a debris flow path. The following points are drawn to summarize the study outcome:

1. The test result show F_r values ranging from 4.7 to 9.7 that is higher than what is observed in real debris flow in nature, i.e. $F_r < 3$. This is because the test was made by a natural sand aggregate with water on a smooth flume channel without scaling the viscosity. However, the results followed the power-function relationship that might be useful in extrapolating the results into the field cases.
2. The fine content of the debris material and water content through C_s are seen to affect F_r by controlling v and h_{Max} . This also reflected on the computed slightly higher values of P_{norm} .
3. Better relationship of the recorded impact force with discharge per unit width is found when using an equation derived from momentum balance than the empirical relationship between recorded impact force with the corresponding unit discharge.
4. This impact force measuring method replicates the behaviour of debris flow interacting with passable structures and it can be used to estimate the impact force on energy dissipating structures like slit dams and baffle walls or even bridge (underpass) piers. The installation method is simple and suitable for repetitive tests. It also avoids direct contact of debris with the load cell that could damage it.

6 ACKNOWLEDGEMENTS

This study was supported financially by the Norwegian Public Roads Administration (NPRA) E39 ferry-free highway project. The authors are grateful for the help from Einar Husby, Espen Andersen, Karl Ivar Volden Kvisvik, Per A. Østensen, Frank Stæhli in building and instrumenting the flume model.

7 REFERENCES

- Arattano, M, and L Franzi. 2003. "On the Evaluation of Debris Flows Dynamics by Means of Mathematical Models." *Natural Hazards and Earth System Science* 3 (6):539–44.
- Armanini, Aronne. 1997. "On the Dynamic Impact of Debris Flows." In *Recent Developments on Debris Flows*, edited by Aronne Armanini and Masanori Michiue, 208–26. Berlin, Heidelberg: Springer.
- Cui, Peng, Chao Zeng, and Yu Lei. 2015. "Experimental Analysis on the Impact Force of Viscous Debris Flow." *Earth Surface Processes and Landforms* 40 (12):1644–55.
- Huang, Hung-Pin, Kai-Chun Yang, and Shao-Wun Lai. 2007. "Impact Force of Debris Flow on Filter Dam." *Momentum* 9 (2):3218.
- Hübl, Johannes, and Gerhard Holzinger. 2003. "Development of Design Basis for Crest Open Structures for Debris Flow [in German]." Vienna.
- Hübl, Johannes, Jürgen Suda, Dirk Proske, Roland Kaitna, and Christian Scheidl. 2009. "Debris Flow Impact Estimation." In *International Symposium on Water Management and Hydraulic Engineering*, 137–48. Macedonia.
- Iverson, Richard M. 1997. "The Physics of Debris Flows." *Reviews of Geophysics* 35 (3). Wiley-Blackwell:245–96.
- Mizuyama, T. 1979. "Computational Method and Some Considerations on Impulsive Force of Debris Flow Acting on Sabo Dams [in Japanese]." *Journal of the Japan Society of Erosion Control Engineering* 32 (1):40–43.
- Nagl, G., R. Kaitna, and J. Hübl. 2018. "A Monitoring Barrier for Investigating Debris Flow/Structure/Ground Interactions." In *5th International Conference on Debris Flows: Disasters, Risk, Forecast, Protection*, edited by S. S. Chernomorets and G. V. Gavardashvili, 152–57. Tbilisi, Georgia: Publishing House "universal."
- Scheidl, Christian, Michael Chiari, Roland Kaitna, Matthias Müllegger, Alexander Krawtschuk, Thomas Zimmermann, and Dirk Proske. 2013. "Analysing Debris-Flow Impact Models, Based on a Small Scale Modelling Approach." *Surveys in Geophysics*.
- Song, D., C. W. W. Ng, C. E. Choi, G. G. D. Zhou, J. S. H. Kwan, and R. C. H. Koo. 2017. "Influence of Debris Flow Solid Fraction on Rigid Barrier Impact." *Canadian Geotechnical Journal* 54:1421–33.
- Tibergien, D, D Laigle, M Naaïm, E Thibert, and F Ousset. 2007. "Experimental Investigations of Interaction between Mudflow and an Obstacle." In *Debris-Flow Hazards Mitigation: Mechanics, Prediction and Assessment*, edited by C. L. Chen and J.J. Major, 681–87. Millpress.
- Wang, Dongpo, Zheng Chen, Siming He, Yang Liu, and Hao Tang. 2018. "Measuring and Estimating the Impact Pressure of Debris Flows on Bridge Piers Based on Large-Scale Laboratory Experiments." *Landslides* 15 (7). Springer Berlin Heidelberg:1331–45.
- Wang, Youbiao, Xiaofeng Liu, M Asce, ; Changrong Yao, Yadong Li, Saizhi Liu, and Xun Zhang. 2018. "Finite Release of Debris Flows around Round and Square Piers." *Journal of Hydraulic Engineering* 44 (12).
- Yifru, A.L., R.N. Pradhan, S. Nordal, and V. Thakur. 2018. "Preliminary Study of Debris Flow Impact Force on a Circular Pillar." In *Physical Modelling in Geotechnics (ICPMG 2018)*, Volume 2, edited by Andrew McNamara and Sam Divall, 1105–10. London: CRC Press.
- Zanutigh, Barbara, and Alberto Lamberti. 2006. "Experimental Analysis of the Impact of Dry Avalanches on Structures and Implication for Debris Flows." *Journal of Hydraulic Research* 44 (4). Taylor & Francis Group:522–34.
- Zhang, Shucheng. 1993. "A Comprehensive Approach to the Observation and Prevention of Debris Flows in China." *Natural Hazards* 7 (1):1–23.